PCCP

Direct comparison between subnanometer hydration structures on hydrophilic and hydrophobic surfaces via three-dimensional scanning force microscopy

Journal:	*Physical Chemistry Chemical Physics*
Manuscript ID	CP-ART-04-2018-002309.R1
Article Type:	Paper
Date Submitted by the Author:	27-Jun-2018

Complete List of Authors:	Yang, Chih-Wen; Academia Sinica, Institute of Physics Miyazawa, Keisuke; Kanazawa University, Fukuma, Takeshi; Kanazawa University, Miyata, Kazuki; Kanazawa University Hwang, Ing-Shouh; Academia Sinica, Institute of Physics

PCCP

Article

Direct comparison between subnanometer hydration structures on hydrophilic and hydrophobic surfaces via three-dimensional scanning force microscopy†

Received 00th January 20xx,
Accepted 00th January 20xx

DOI: 10.1039/x0xx00000x

www.rsc.org/

Chih-Wen Yang[a], Keisuke Miyazawa[b], Takeshi Fukuma*[b,c], Kazuki Miyata[b], Ing-Shouh Hwang*[a]

Investigating interfacial water ordering on solid surfaces with different hydrophobicities is fundamentally important. Here, we prepared hydrophilic mica substrates with some areas covered by mildly hydrophobic graphene layers, and studied the resulting hydration layers using three-dimensional (3D) force measurements based on frequency-modulation atomic force microscopy. Hydration layers of 0.3-0.6 nm were detected on bare graphene regions; these layers were considerably larger than the spacing measured on mica (0.2-0.3 nm). On the graphene-covered regions, we also observed formation of special ordered structures of adsorbates over time, on which, surprisingly, no prominent hydration layers were detected. Based on these findings, we present one possible scenario to describe the formation process of the ordered interfacial structures and the enhanced oscillation period in the force profiles. This work also demonstrates the capability and significance of 3D force measurements in probing hydration behaviors on a heterogeneous substrate with a lateral resolution smaller than several nanometers.

Introduction

Characterization of solid-liquid interfaces is of crucial importance for exploring a wide range of naturally occurring and technological phenomena, such as the solid-electrolyte interfaces in batteries,[1,2] bio-molecular adsorption,[3-5] the control of colloidal systems,[6,7] and liquid slippage at hydrophobic walls.[8-10] Of particular interest is the behavior of liquid water in contact with solid surfaces, which has been a fundamental subject of numerous studies for understanding the solid-liquid interfacial phenomena.[11,12] At interfaces between hydrophilic solids and water (hydrophilic-water interfaces), water molecules usually rearrange to form layer-like structures (hydration layers) or a tightly structured distribution at a flat solid surface. Dynamic atomic force microscopy (AFM) has been used to measure oscillatory hydration forces at hydrophilic-water interfaces with a period of 0.20-0.30 nm.[13-22]

It is not clear whether hydration layers also form at the interfaces between hydrophobic solids and water (hydrophobic-water interfaces) because very few AFM studies have been performed on this type of interfaces so far. Using frequency-modulation AFM (FM-AFM), two research groups reported that hydration layers also form at graphite-water interface.[20,21] Their measurements of resonance frequency shift versus tip-sample separation reveal an oscillation period of 0.3-0.4 nm, which was larger than the measurements conducted at hydrophilic-water interfaces. However, Gillian et al. reported no oscillation at hydrophobic-water interfaces using a hydrophilic or a hydrophobic tip.[19] Schlesinger et al. used hydrophobic tips to study hydrophobic surfaces, perfluorodecyltrichlorosilane (FDTS) monolayers and highly *oriented pyrolytic graphite* (HOPG), in water. A portion of the measured force curves (resonance frequency shift vs tip-sample separation) exhibit an oscillation periodicity of ~0.5 nm when the tip approaches within ~1.5 nm of the hydrophobic surfaces, but

[a] *Institute of Physics, Academia Sinica, 11529, Taipei, Taiwan. E-mail: ishwang@phys.sinica.edu.tw.*
[b] *Division of Electrical Engineering and Computer Science, Kanazawa University, Kakuma-machi, Kanazawa 920-1192, Japan. E-mail: fukuma@staff.kanazawa-u.ac.jp*
[c] *Nano Life Science Institute (WPI-NanoLSI), Kanazawa University, Kakuma-machi, Kanazawa 920-1192, Japan*

† Electronic Supplementary Information (ESI) available: Height image and 3D △f mapping on graphene-covered area in DI water, typical force curves of frequency shift versus the tip position measured on bare graphene.
See DOI: 10.1039/x0xx00000x

other force curves do not exhibit oscillation.[22] It remains unclear why oscillatory force curves are detected in some measurements but not in others. Also, it is puzzling why the separation of two neighboring hydration layers can be considerably larger than the size of a water molecule. In these studies, one cannot rule out the possible effects of the tip on the force curve measurements because only a single type of solid-water interfaces (hydrophilic-water or hydrophobic-water) is prepared for the force-curve measurements. Thus, there is a need to prepare a sample with hydrophilic and hydrophobic regions simultaneously present on the solid surface, so that the same tip can be used to make the force-curve measurements on both hydrophilic and hydrophobic areas in water.

In this work, we used custom-built, highly sensitive, low-noise two-dimensional (2D) FM-AFM[23-26] and 3D scanning force microscopy (3D-SFM)[16,17] to study a hydrophilic mica substrate with some areas covered by mildly hydrophobic graphene layers in pure water. 3D-SFM enabled us to measure force curves on areas of different structures with a lateral resolution of several nanometers down to the atomic scale. This unique capability to characterize the structures of interfacial water provides measurements that can be directly compared with current theoretical calculations. 3D-SFM also complement other macroscopic, spectroscopic, and microscopic measurements of solid-water interfaces, particularly in characterizing heterogeneous interfaces. Combining these experimental and theoretical studies will improve fundamental understanding of solid-water interfaces in general and resolve numerous mysteries related to the interfaces.

Our measurements showed that the oscillation period on bare graphene areas was considerably larger than that on mica, indicating that larger oscillation periodicity is intrinsic to the hydrophobic-water interfaces, rather than an effect caused by the tip. On the graphene-covered areas, we also observed domains of ordered structures of adsorbates. Interestingly, the force curves measured on the ordered structures did not exhibit the oscillatory behavior seen on bare graphene regions, perhaps explaining why some previous studies did not observe any oscillation at hydrophobic-water interfaces. Because the oscillation periodicity in the force curve measured on bare graphene was very close to the height of the ordered structures, the larger oscillatory hydration layers may be related to the formation process of the ordered structures. This experimental study and our proposed mechanism provide crucial information for understanding water ordering around hydrophobic surfaces (hydrophobic hydration), which may help to identify the origin of intrinsic hydrophobic interaction.

Experimental

Sample Preparation. A mica substrate with small areas covered by graphene flakes was prepared right before each atomic force microscopy (AFM) measurement. The preparation procedure is illustrated in Fig. 1a, which is similar to a previous work.[27] The topmost layers of two mica plates (Ted Pella 50-12, 12 mm × 12 mm) and a highly *oriented pyrolytic graphite* (HOPG) sample (lateral size of 12 mm × 12 mm, ZYB; Momentive) were first peeled off with Scotch tape to expose their clean surfaces. A small piece of a thin graphite flake was carefully removed from the HOPG surface with tweezers and placed on the cleaved surface of a mica plate. The freshly cleaved side of the other mica plate was pressed strongly against the graphite flake by hand for ~1 min. Then, the graphite flake was removed from the bottom mica substrate with tweezers. The samples were examined using optical microscopy and then placed in a liquid cell of our home-made AFM. Two examples are shown in Figs. 1b and c. Thick graphite flakes remained, but few-layer graphene can often be found at the boundaries with mica. Approximately 100 µl of deionized water (purified using a Milli-Q system; resistivity of 18.2 Ω·cm) was injected into the open liquid cell for AFM in a liquid environment.

AFM Experiments. We adopted frequency-modulation (FM) detection for our AFM measurements, which has been demonstrated to achieve sufficient force sensitivity to detect hydration layers.[15,28] We used a custom-built FM-AFM with an ultra-low noise cantilever detection sensor and a high stability photothermal excitation system[25,26]. The AFM head was controlled with a commercially available AFM controller (ARC2, Asylum Research). A cantilever was oscillated at a constant amplitude using a commercially available oscillation controller (OC4, SPECS). In the FM detection scheme, the tip-sample interaction was detected as a resonance frequency shift (Δf) of the vibrating cantilever. We first performed 2D mapping with a constant frequency shift to regulate the Z distance of the tip for obtaining the surface topography. On selected areas, 3D Δf measurements[16,17] were conducted to investigate the local distribution of hydration layers. In our 3D Δf

mapping, a tip was scanned in Z as well as in XY to cover the whole 3D interfacial space. For the scan in Z, a small vertical vibration was modulated with a sine wave faster than the bandwidth of the Z distance regulation while the tip was laterally scanned. During the 3D Δf mapping, Δf was recorded in real time with respect to the 3D tip positions, while the averaged tip height was regulated to keep the averaged dissipation constant. The 3D Δf image was constructed from either approaching or retracting Z profiles at each XY positions and the 2D height image could be obtained simultaneously. We employed dissipation, rather than the frequency shift, as the feedback signal in regulating the Z height because the change of dissipation versus tip-sample distance is monotonic, thus stable imaging of a large scan area, particularly across the boundary of graphene and mica surfaces, could be achieved.

From our 3D Δf mapping, we derived Z-section images to identify the correlation between the force-distance curve and the height at different positions. We used small Si cantilevers (AC55, Olympus) with MHz-resonance to enhance the force sensitivity. Photothermal-actuation was used to excite pure resonance of the AFM cantilever in water. [25,26] Before each AFM measurement, the tip apex was rendered hydrophilic by coating with a Si film of 30 nm using a dc sputter coater (K575XD, Emitech). [26,29] In our experiments, it usually took an hour to optimize the operation of FM-AFM and to engage the tip to the sample surface.

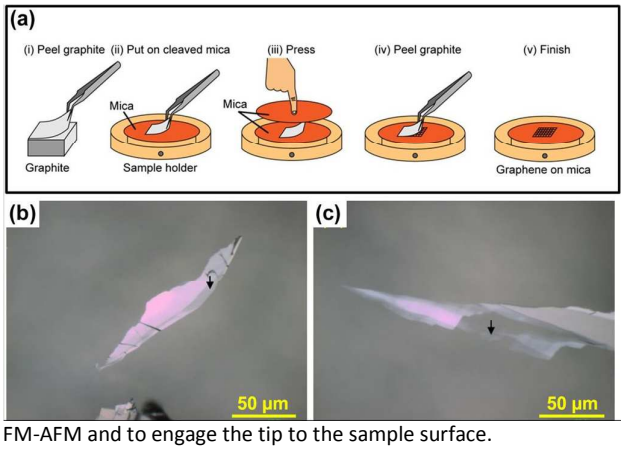

Fig. 1 Optical images of mica with graphene-covered regions. (a) Schematic showing the procedure for depositing graphene flakes on mica substrates. (b) Optical image of the sample for Fig. 2. The black arrow indicates the position for AFM study. (c) Optical image of the sample for Fig. 3. The black arrow indicates the position for AFM study

Results and discussion

AFM measurements on mica and a graphene-covered area in DI water

In our AFM measurements, we first acquired topographic images to identify the flat mica regions and the graphene-covered regions. **Fig. 2a** shows a height image of a graphene-covered area acquired ~1 hr after a sample was immersed in deionized water. A portion of the graphene surface of our sample was covered by row-like ordered structures of adsorbates. The height of the ordered structure was ~0.5 nm. The appearance of the ordered structures and the gradual increase in their coverage on the graphene surface over time are similar to previous AFM observations on HOPG in pure water. [30-35] We also performed 3D Δf mapping on a selected area (red square in Fig. 2a). The height (Fig. 2b) and the corresponding force curves of resonance frequency shift versus the tip-sample separation were obtained simultaneously. Fig. 2c depicts the Z-section profile along the red dashed line in Fig. 2b obtained from the 3D Δf map. Contrast of periodic oscillation was evident in only a certain area, which was lower in height and corresponded to a bare graphene region. When the force curves were averaged over the outlined regions on bare graphene and on ordered structures of adsorbates in Fig. 2c, no clear oscillation in the force curve was detected on the ordered structures, but oscillation was evident on bare graphene (Figs. 2d, e).

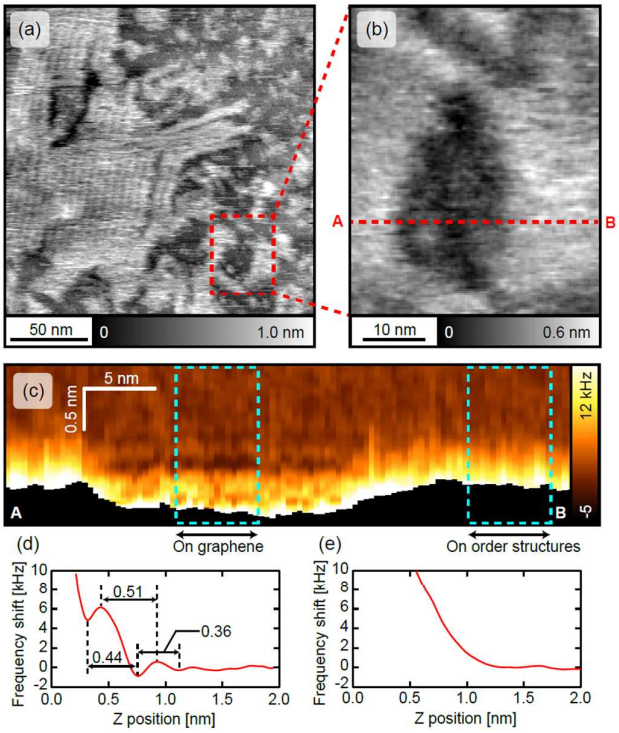

Fig. 2 AFM measurements revealing the heterogeneous nature of a graphene-covered area in pure water. (a) Topographic image. Brighter areas are ordered structures of adsorbates. (b) Height image obtained from 3D Δf mapping performed in the area outlined by the red square in (a). (c) Z-section profile along the red dashed line in (b). (d) and (e) Force curves averaged over the outlined regions on bare graphene and on ordered structures in (c), respectively. The working frequency of the cantilever was ~ 1.3 MHz, the working amplitude was ~ 0.11 nm, and Q~ 10.4.

Fig. 3a shows a topographic image of a region with mica on the left side and a graphene-covered region on the right. The mica exhibited an atomically flat surface, and the multi-layer graphene had a thickness of ~5 nm. Most of the areas on graphene were covered by the ordered structures of adsorbates.[36] Fig. 3b depicts a Z-section profile from a 3D Δf map measured along the red dashed line in Fig. 3a. Oscillation related to the hydration layers on mica (to the left of the graphene step edge) was visible. On graphene (to the right of the graphene step edge), oscillation of a larger periodicity was seen only on small regions corresponding to bare graphene. Figs. 3c and d show that the oscillation period in the force curves measured on graphene is larger than that on mica. We also selected a small region on mica as well as on a small bare graphene region to acquire 3D Δf maps. Figs. 3e and f show two Z-section profiles of 3D Δf maps acquired on a mica area and on a bare graphene area, respectively (Fig. 3a). The oscillation period in the frequency-shift on bare graphene was approximately twice of the period on mica. Figs. 3g and h show the force curves averaged over the outlined regions in Figs. 3e and f, respectively. The period of the hydration layers on mica was 0.26-0.33 nm, which matches measurements in previous studies.[12,14-17,22] In contrast, the period on bare graphene was 0.5-0.6 nm.

Fig. S1a† shows a topographic image of an approximate area seen in Fig. 3a. We performed 3D Δf mapping in the area outlined by a red dashed square. Fig. S1b† is the height image obtained from that 3D Δf mapping and Fig. S1c† is the Z-section profile along the red dashed lines in Fig. S1b†. Oscillations were visible only on the bare graphene, similar to the results in Fig. 2c. We performed similar measurements on four graphene-covered mica samples and all of the 3D Δf measurements exhibited hydration behaviors similar to those presented in this work (data not shown).

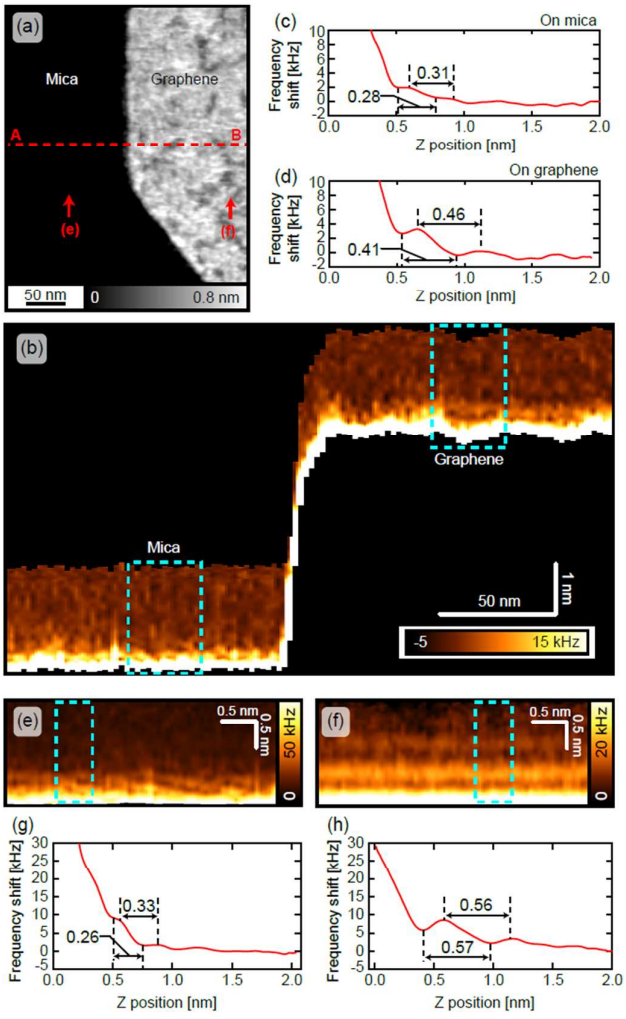

Fig. 3 AFM measurements with a single tip on an area with both mica and a graphene-covered region. (a) Topographic image. (b) Z-section profile of a 3D Δf map across a boundary along the dashed red line in (a). (c) and (d) Force curves averaged over the dashed outlined regions on a mica region (c) and a bare graphene region (d) in (b). (e) and (f) Z-section profiles of 3D Δf maps acquired at a mica area (e) and at a bare graphene area (f) in (a). (g) and (h) Force curves averaged over the dashed outlined regions in (e) and (f), respectively. The working frequency was ~ 1.3 MHz, Working amplitude was ~ 0.11 nm, and Q~ 10.4.

In 3D Δf mapping, only 256 points were acquired in each force-curve measurement in order to achieve a sufficiently short data-acquisition time in each mapping. We also acquired high-resolution force curve of the frequency shift versus the tip-sample distance at selected sites in pure mica areas, bare graphene areas, and adsorbate-covered graphene areas (Figs. 4a-c). We measured the oscillation with a period of 0.20-0.25 nm next to the mica substrate (Fig. 4a). A weaker oscillation with a period of ~0.5 nm was detected above a bare graphene area (Fig. 4b); similar force-curve measurements are shown in Fig. S2†. A nearly monotonic increase in the force curve with no obvious oscillation in the frequency shift was seen on an ordered structure on graphene (Fig. 4c). These measurements are consistent with those obtained via 3D Δf mapping (Figs 2 and 3). Fig. 4d illustrates a schematic of the water layer structures based on our measurements.

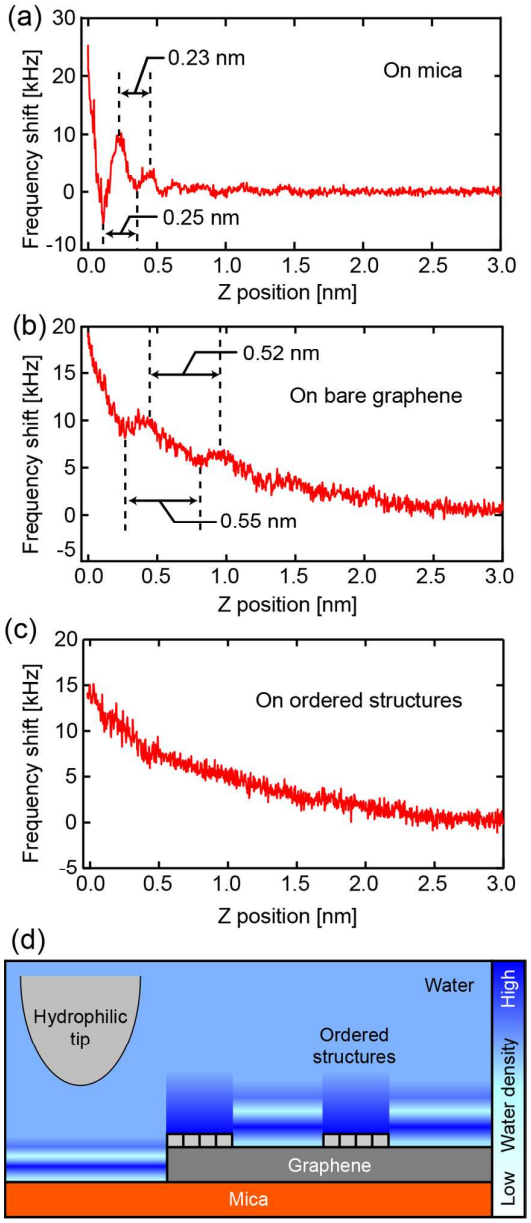

Fig. 4 (a) High-resolution one-dimensional (1D) force-curve measured on mica; (b) High-resolution 1D force curve measured on bare graphene. (c) High-resolution 1D force curve measured on an ordered structure of adsorbates. (d) Schematic of water layering on mica, bare graphene, and adsorbate-covered graphene regions.

Our 3D Δf mappings and 1D force curve measurements consistently indicated that the thickness of the hydration layers on bare graphene was 0.3-0.6 nm, which is considerably larger than the hydration layer of 0.2-0.3 nm measured on mica. In addition, no prominent water layering was detected on the ordered structures on graphene. Here we used the same hydrophilic tip to detect these distinct features of interfacial water. Suzuki et al. and Utsunomiya

et al. also detected hydration layers of 0.3-0.4 nm on HOPG substrates.[20,21] Schlesinger and Sivan detect hydration layers of ~0.5 nm on two hydrophobic substrates (HOPG and FDTS monolayer) using hydrophobic tips. Thus, the large spacing in the hydration layers next to the graphene (as well as HOPG and FDTS monolayer) surface is probably an intrinsic property of the interfacial water, rather than an effect caused by the tip or by confinement between the tip and the sample. To understand whether this feature is general to most hydrophobic surfaces, it is highly desirable to perform AFM of hydration forces on many more hydrophobic substrates.

Why can water arrange into layers with a thickness nearly twice the size of a water molecule on hydrophobic substrates? Schlesinger and Sivan proposed the existence of partially ordered layers of hydrated gas near the hydrophobic surface.[22] We agree that the large hydration layer may contain dissolved nitrogen and oxygen molecules, because AFM-based studies previously indicated that dissolved air gas tend to segregate at hydrophobic-water interfaces, forming a variety of interfacial structures.[30-35] In the current study, we used deionized water, which has a dissolved air gas concentration slightly below the saturation level. Previous AFM studies of HOPG-water interfaces suggested that dissolved nitrogen molecules may accumulate at the interface and form ordered row-like structures gradually over tens of minutes or hours.[30-35] The ordered structures and their formation dynamics are very similar to the observations of adsorbate structures on graphene in this work. Because the thickness of the row-like structures is similar to the spacing of hydration layers measured above the bare graphene areas, we speculate that they are related phenomena occurring at the graphene-water interface.

Molecular dynamic simulations have indicated that water can form a dynamic clathrate-like cage around a small hydrophobic molecule[37]. A previous AFM-based study suggested that the ordered structures at HOPG-water interfaces may constitute an interfacial gas hydrate phase.[34] We therefore propose the following scenario. Before stable ordered row-like structures form atop the sample surface, dissolved nitrogen and oxygen molecules may become enriched near the graphene-water interface, reducing the interfacial tension between water and graphene (a hydrophobic surface). The interfacial water may form a clathrate-like cage around individual nitrogen or oxygen molecules, but the structures are highly dynamic. Interactions among water, the flat graphene surface, and dissolved gas molecules lead to the formation of layer-like structures. Occasionally, the dynamic clathrate-like layer structures may form small domains of a 2D ordered structure commensurate with one crystal orientation of the graphene (or HOPG) lattice. The ordered interfacial gas clathrate structures are relatively stable and can serve as a nucleus for further growth of the domains. This scenario explains the observations of hydration layers with large periods and the formation of ordered structures on graphene or graphite surfaces in water. Further experimental and theoretical investigations are required to interrogate the proposed scenario.

Hydrophobic interactions play a central role in the self-assembly of biological molecules and hydrophobic particles in water, but the origin and nature of intrinsic hydrophobic interactions remain unknown.[38,39] Experimental investigation of hydrophobic hydration will provide crucial information to identify the origin of hydrophobic interactions. Our FM-AFM measurements suggest that dissolved nitrogen and oxygen molecules in the hydration layers may contribute to intrinsic hydrophobic interaction.[40]

Our 3D Δf measurements clearly indicate that no prominent hydration layers form above the ordered structures, which has important implications on two aspects. First, it explains why some of previous AFM force measurements did not reveal oscillations at hydrophobic-water interfaces.[19,22] Second, this feature is very surprising because hydration on the ordered structures does not behave like that on typical hydrophilic substrates, which exhibit a more tightly structured or ordered water distribution than a hydrophobic surface. It also differs from the thick hydration layers seen on hydrophobic substrates such as HOPG[20-22], graphene, and FDTS[22] monolayer. Formation of the ordered structures modifies the local surface chemistry of the hydrophobic substrate; ordering of water above the surface changes as well. This behavior reveals an intriguing phenomenon that renders hydrophobic-water interfaces more heterogeneous and complicated over time. Further investigations of hydrophobic-water interfaces should consider such a phenomenon. Further investigation is needed to determine the nature and detailed molecular structures of the ordered row-like structures experimentally and theoretically.

It was reported that many graphitic surfaces may become more hydrophobic due to contamination from airborne hydrocarbon.[41] Whether the ordered row-like structures are caused by adsorption of airborne hydrocarbon have been discussed in previous studies.[30,33] In addition, previous works have shown that formation of the ordered row-like structures is strongly related to the concentration of nitrogen and oxygen dissolved in water.[27,30-35] Furthermore, water protects graphitic surface from airborne hydrocarbon contamination.[42] Thus, it is very unlikely that the ordered structures are caused by hydrocarbon accumulation on graphitic surfaces.

Conclusions

Currently, investigations of surface hydrophobicity (or surface wetting properties) mainly rely on water contact angle (WCA) measurements, which are taken over a lateral dimension of 1 mm or larger. Surface defects and heterogeneities such as step edges, impurities, and adsorbates are nearly unavoidable on interfaces at this macroscopic scale, affecting WCA values. However, the results obtained from WCA measurements have been widely adopted for comparison with theoretical simulations and calculations, which typically assumes the contact of pure water with solid surfaces of a lateral dimension of a few nanometres at most. In this work, we demonstrated that 3D Δf measurements can characterize the local hydration behaviors on heterogeneous substrates with a spatial resolution of several nanometers or smaller, which should be more suitable for comparison with theoretical simulations or calculations. Combining such microscopic characterization methods with theoretical studies may lead to fundamental understanding of water-solid interfaces.

Acknowledgements

We thank the Ministry of Science and Technology (MOST 106-2112-M-001-025-MY3) of the Republic of China, and Academia Sinica for supporting this study. This work was also supported by ACT-C, Japan Science and Technology Agency, JSPS KAKENHI (No. JP16H02111), and CHOZEN Project, Kanazawa University.

Notes and references

1 B. M. Winter, J. O. Besenhard, M. E. Spahr, P. Novμk, *Adv. Mater*. 1998, **10**, 725-763.

2 P. Poizot, S. Laruelle, S. Grugeon, L. Dupont, J. Tarascon, *Nature* 2000, **407**, 496–499.

3 Z. Wu, X. Zhang, X. Zhang, G. Li, J. Sun, Y. Zhang, M. Li, J. Hu, *Surf. Interface Anal.* 2006, **38**, 990–995.

4 Z. Wu, X. Zhang, X. Zhang, J. Sun, Y. Dong, J. Hu, *Chinese Science Bulletin* 2007, **52**, 1913-1919.

5 M. Holmberg, A. Ku¨ hle, J. Garnæs, K. A. Mørch, A. Boisen, *Langmuir* 2003, **19***,* 10510-10513.

6 M. I. Smith, *Sci. Rep.* 2015, **5**, 14175.

7 D. R. E. Snoswell, J. Duan, D. Fornasiero, J. Ralston, *J. Phys. Chem. B* 2003, **107,** 2986-2994.

8 C. Cottin-Bizonne, J.-L. Barrat, L. Bocquet, E. Charlaix, *Nature Materials* **2** 2003, 237–240.

9 Y. Wang, B. Bhushan, *Soft Matter* 2010*,* **6**, 29–66.

10 A. Steinberger, C. Cottin-Bizonne, P. Kleimann, E. Charlaix, *Nature Materials* 2007, **6**, 665−668.

11 D. Argyris, N. R. Tummala, A. Striolo, D. R. Cole, *J. Phys. Chem. C* 2008, **112***,* 13587–13599.

12 L. Cheng, P. Fenter, K. L. Nagy, M. L. Schlege, N. C. Sturchio, *Phys. Rew. Lett*. 2001, **87**, 156103.

13 J. P. Cleveland, T. E. Schaffer, P. K. Hansma, *Physical Review. B* 1995*,* **52(12)**, R8692-R8695.

14 K. Kimura, S. Ido, N. Oyabu, K. Kobayashi, Y. Hirata, *J. Chem. Phys.* 2010, **132**, 194705.

15 T. Fukuma, K. Kobayashi, K. Matsushige, H. Yamada, *Applied Physics Letters* 2005, **87**, 034101.

16 T. Fukuma, Y. Ueda, S. Yoshioka, H. Asakawa, *Phys. Rew. Lett.* 2010, **104**, 016101.

17 T. Fukuma, *Sci. Technol. Adv. Mater.* 2010, **11**, 033003.

18 M. J. Higgins, M. Polcik, T. Fukuma, J. E. Sader, Y. Nakayama, S. P. Jarvis, *Biophysical Journal* 2006, **91**, 2532-2542.

19 G. B. Kaggwa, P. C. Nalam, J. I. Kilpatrick, N. D. Spencer, S. P. Jarvis, *Langmuir* 2012, **28**, 6589-94.

20 K. Suzuki, N. Oyabu, K. Kobayashi, K. Matsushige, H. Yamada, *Applied Physics Express* 2011, **4**, 125102.

21 T. Utsunomiya, Y. Yokota, T. Enoki, K. Fukui, *Chem. Commun.* 2014, **50**, 15537-15540.

22 I. Schlesinger, U. Sivan, *Langmuir* 2017, ***33***, 2485–2496.

23 T. Fukuma, M. Kimura, K. Kobayashi, K. Matsushige, H. Yamada, *Rev. Sci. Instrum.* 2005, **76**, 053704.

24 T. Fukuma, S. P. Jarvis, *Rev. Sci. Instrum.* 2006, **77**, 043701.

25 T. Fukuma, *Rev. Sci. Instrum.* 2009, **80**, 023707.

26 T. Fukuma, K. Onishi, N. Kobayashi, A. Matsuki, H. Asakawa, *Nanotechnology* 2012, **23**, 135706.

27 H.-C. Ko, W.-H. Hsu, C.-W. Yang, C.-K. Fang, Y.-H. Lu, I.-S. Hwang, *Langmuir*, 2016, ***32***, 11164–11171.

28 T. Uchihashi, M. Higgins, Y. Nakayama, J. E. Sader, S. P. Jarvis, *Nanotechnology* 2005, **16**, S49–S53.

29 S. M. R. Akrami, H. Nakayachi, T. Watanabe-Nakayama, H. Asakawa, T. Fukuma, *Nanotechnology* 2014, **25**, 455701

30 Y.-H. Lu, C.-W. Yang, I.-S. Hwang, *Langmuir* 2012, **28,** 12691−12695.

31 I. -S. Hwang, C.-W. Yang, Y. -H. Lu, *arXiv* 2012*, 1203.6696*.

32 C. -W. Yang, Y. -H. Lu, I. -S. Hwang, *Chin. J. Phys.* 2013, **51**, 174-186.

33 Y. -H. Lu, C. -W. Yang, I. -S. Hwang, *Appl. Surf. Sci.* 2014, **304**, 56-64.

34 Y. -H. Lu, C. -W. Yang, C. -K. Fang, H. -C. Ko, I. -S. Hwang, *Sci. Rep.* 2014, **4**, 7189.

35 C.-K. Fang, H.-C. Ko, C.-W. Yang, Y.-H. Lu, I.-S. Hwang, *Sci. Rep.* 2016, **6**, 24651.

36 The considerably higher adsorbate coverage for the sample shown in Fig. 3a compared with the sample in Fig. 2a arose because it took longer (2 hrs) to scan a very large area of the surface before we reached an area with the boundaries between mica and a graphene-covered region. Coverage of the adsorbate structures grew over this period of time.

37 M. Montagna, F. Sterpone, L. Guidoni, *J. Phys. Chem. B* 2012, **116**, 11695–11700.

38 E. E. Meyer, K. J. Rosenberg, J. Israelachvili, *PNAS* 2006, **103**, 15739-15746.

39 P. Ball, *PNAS* 2017, **114**, 13327-13335.

40 Hydrophobic interactions are attractive forces that cause hydrophobic molecules or surfaces to aggregate in water.[38] These forces can be largely categorized as long-range hydrophobic attraction and intrinsic hydrophobic interaction. Several mechanisms, including bridging surface nanobubbles, electrostatic or dipole interactions, etc., have been used to account for the long-range attraction. It is believed that there is an intrinsic hydrophobic interaction that works in a distance of only several nm or smaller,[38] but its origin and nature remain elusive.

41 Z. Li, Y. Wang, A. Kozbial, G. Shenoy, F. Zhou, R. McGinley, P. Ireland, B. Morganstein, A. Kunkel, S. P. Surwade, L. Li, H. Liu, *Nat. Mater.* 2013, **12**, 925−931.

42 Z. Li, A. Kozbial, N. Nioradze, D. Parobek, G. J. Shenoy, M. Salim, S. Amemiya, L. Li, H. Liu, *ACS Nano* 2016, **10 (1)**, 349.